# Metastable structures and refolding kinetics in hok mRNA of plasmid R1

J. H. Nagel, A. P. Gultyaev, K. Gerdes and C. W. Pleij

*RNA* 1999 5: 1408-1418

*RNA* (1999), *5*:1408–1419. Cambridge University Press. Printed in the USA.


# Metastable structures and refolding kinetics in *hok* mRNA of plasmid R1

**J.H.A. NAGEL,[1] A.P. GULTYAEV,[1,2] K. GERDES,[3] and C.W.A. PLEIJ[1]**

[1]Leiden Institute of Chemistry, Gorlaeus Laboratories, 2300 RA Leiden, The Netherlands
[2]Section Theoretical Biology and Phylogenetics, Institute of Evolutionary and Ecological Sciences, Leiden University, 2311 GP Leiden, The Netherlands
[3]Department of Molecular Biology, Odense University, Dk-5230, Odense M, Denmark

## ABSTRACT

**Programmed cell death by *hok*/*sok* of plasmid R1 and *pnd*/*pndB* of R483 mediates plasmid maintenance by killing of plasmid-free cells. It has been previously suggested that premature translation of the plasmid-mediated toxin is prevented during transcription of the *hok* and *pnd* mRNAs by the formation of metastable hairpins in the mRNA at the 5′ end. Here, experimental evidence is presented for the existence of metastable structures in the 5′ leader of the *hok* and *pnd* mRNAs in vitro. The kinetics of refolding from the metastable to the stable structure in the isolated fragments of the 5′ ends of both the *hok* and *pnd* mRNAs could be estimated, in agreement with the structural rearrangement in this region, as predicted to occur during transcription and mRNA activation. The refolding rates of *hok* and *pnd* structures are slow enough to allow for the formation of downstream hairpin structures during elongation of the mRNAs, which thereby helps to stabilize the metastable structures. Thus, the kinetic refolding parameters of the *hok* and *pnd* mRNAs are consistent with the proposal that the metastable structures prevent premature translation and/or antisense RNA binding during transcription.**

**Keywords: branch migration; kinetic traps; RNA rearrangements; RNA refolding; strand displacement; structure probing**

## INTRODUCTION

Transient structures in RNA can be functionally important, as the final structure of an RNA often depends on a specific folding pathway determined by the RNA itself (LeCuyer & Crothers, 1993; Franch et al., 1997; Gultyaev et al., 1997; Cao & Woodson, 1998). These transient structures in RNA play a very important role in the *hok*/*sok* system of plasmid R1, which is the paradigm member of the gene family. This *hok*/*sok* system mediates plasmid maintenance by killing plasmid-free cells via a complex series of mRNA rearrangements (Gerdes et al., 1986; Franch et al., 1997). The *hok*/*sok* system codes for a stable mRNA that folds via a complicated pathway into the active structure. This active structure leads to the synthesis of the toxic Hok (Host killing) protein, which, if expressed, kills the cell (Franch et al., 1997; Gultyaev et al., 1997).

To prevent translation of the Hok toxin in the cell, the full-length stable *hok* mRNA is locked into an inactive conformation by the *fbi* (folding back inhibitory) element (Thisted et al., 1995; Franch & Gerdes, 1996). This *fbi* element is located at the extreme 3′ end and binds to the extreme 5′ end of the *hok* mRNA, the *tac* (translation activation) element (Fig. 1B; Thisted et al., 1994a; Nielsen & Gerdes, 1995; Franch & Gerdes, 1996). This interaction blocks the formation of the complete *tac* stem at the 5′ end and thereby holds the $SD_{mok}$ (Shine-Dalgarno; modulation of killing) inaccessible to ribosomes. Thus, the expression of the Hok toxin is prevented, because the translation of *hok* is coupled to that of *mok* (Thisted & Gerdes, 1992).

This full-length *hok* mRNA is stable and forms a pool of inactive mRNAs. In time, however, the full-length mRNA gets processed from the 3′ end removing the *fbi* sequence and unlocking the 5′ end *tac* sequence (Fig. 1B,C). This truncation leads to a refolding of the mRNA into its active conformation by the formation of the complete *tac* stem in which the *tac* sequence interacts with the *ucb* (upstream complementary box) region (Fig. 1C; Franch et al., 1997; Gultyaev et al., 1997). The structural rearrangement in the truncated *hok* mRNA leads to the opening of two sites, the $SD_{mok}$ sequence and the *sok target* site (*sokT*). The opening of the $SD_{mok}$ sequence activates the *hok* mRNA because ribosomes can now bind. Killing, however, is pre-

Reprint requests to: C.W.A. Pleij, Leiden Institute of Chemistry, Gorlaeus Laboratories, Einsteinweg 55, 2300 RA Leiden, the Netherlands; e-mail: C.Pley@chem.LeidenUniv.nl.

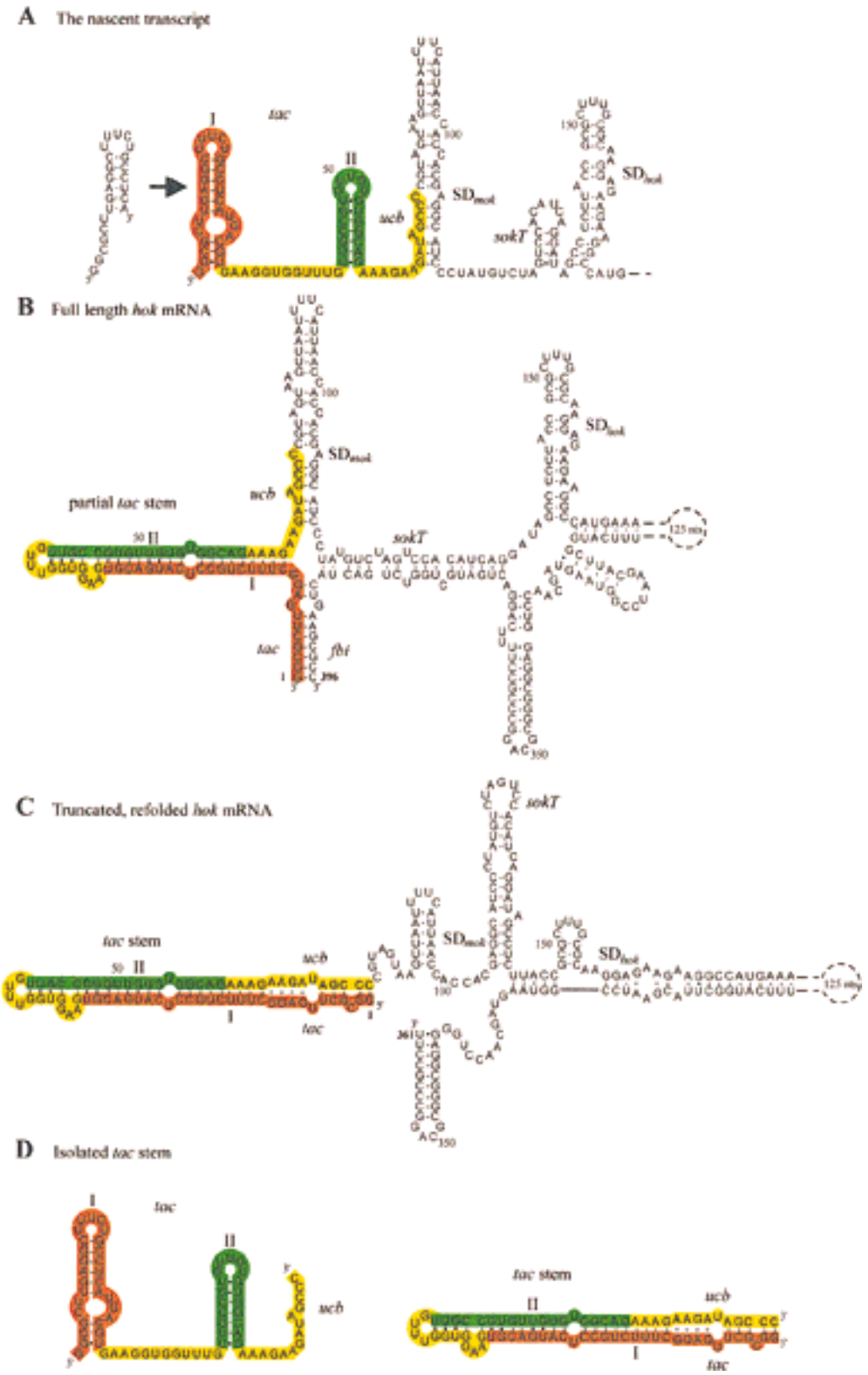


**FIGURE 1.** The folding pathway of *hok* mRNA with the position of the metastable hairpin I shown in orange, the position of the metastable hairpin II shown in green, and the remainder of the isolated *tac* stem shown in yellow. **A**: During the transcription of the *hok* mRNA, it first forms the metastable hairpins at the 5′ end that are stabilized by the *ucb*/SD$_{mok}$ interaction. **B**: After complete transcription of the full-length *hok* mRNA, a refolding takes place, disrupting the metastable hairpins by forming the partial stable *tac* stem with the *tac*/*fbi* interaction while maintaining the *ucb*/SD$_{mok}$ base pairing. **C**: The full-length *hok* mRNA is processed at its 3′ end. The processing triggers a refolding of the mRNA into the active conformation by forming the complete stable *tac* stem with the *ucb*/*tac* interaction and the opening of the *sokT* site. **D**: The isolated 74-nt *hok tac* stem RNA fragment.

vented in a plasmid-carrying cell, because an antidote against the active truncated *hok* mRNA is present in the form of the Sok antisense RNA (Suppression of killing RNA) (Thisted et al., 1994b), which is transcribed from the same plasmid as the *hok* mRNA. This antisense RNA can bind to the activated *sokT* on the truncated *hok* mRNA, which leads ultimately to RNase III degradation of the mRNA and thus to prevention of killing (Franch et al., 1997; Gultyaev et al., 1997). In plasmid-free cells, however, the unstable Sok-RNA becomes quickly depleted and cannot be replenished, leaving a pool of activatable full-length *hok* mRNA, which will kill the cell (Gerdes et al., 1986).

The finding of a translational activator or *tac* stem upstream of the translation initiation region in the *hok* mRNA was puzzling, because it poses the question of how translational activation during transcription is prevented. This is especially true because this *tac* stem is in the thermodynamically most stable conformation when the *tac*/*ucb* interaction is present in the absence of 3′ end *fbi* sequence, thus resembling the situation of the truncated active *hok* mRNA (Fig. 1B,C,D). In other words, how is translation blocked during transcription, as the 3′ proximal *fbi* is only present after complete transcription of the *hok* mRNA (Fig. 1B)?

The answer to this question was found in the folding pathways of seven *hok*-homologs, which were simulated by a genetic algorithm (Gultyaev et al., 1995a). The results of these predictions indicated the existence of metastable structures in the *tac* region, which are formed during the transcription of the mRNA (Fig. 1A; Gultyaev et al., 1997). The predicted metastable structures were further supported by the finding of coupled nucleotide covariations, which provide evidence that the *hok* mRNA 5′ end pairs with three different partners during the complex series of RNA rearrangements in the life cycle of the mRNA (Fig. 1). It was proposed that during transcription, the metastable structure formed at the 5′ end prevents the formation of the active stable *tac* stem conformation (*tac*/*ucb* pairing) and may also prohibit Sok-RNA binding (Gultyaev et al., 1997). Upon completion of the transcript, the metastable structures are disrupted in favor of stable pairing between the 5′ end of the *tac* region and the 3′ end of the *fbi* region (Fig. 1B). Thus, the proposed phylogenetically conserved folding pathway suggests the existence of an inactive mRNA structure during transcription followed by a restructuring after completion, giving rise to a structure that is still inactive, and a subsequent activation via posttranscriptional processing (Fig. 1B,C).

In this article we present experimental evidence for the existence of the predicted metastable structure in the *tac* stem region in vitro. To obtain this evidence we studied RNA fragments corresponding to the *tac* stems of *hok* (Fig. 1D) and *pnd* (promotion of nucleic acid degradation), which were analyzed with structure-probing experiments. To determine the secondary structure of the metastable state of these fragments, a kinetic trap had to be used to force the structures into the metastable state. This trapping not only allowed us to probe the metastable structures of the *hok* and *pnd* fragments but, equally important, it allowed us to follow the refolding event from the metastable to the stable states. The observed refolding appears to be sufficiently slow to allow for the formation of downstream hairpins in the mRNAs, which help to stabilize the metastable states in the *tac* stem regions until the complete mRNA is transcribed. After completion of the mRNA, the *fbi* element is able to disrupt the metastable state, allowing it to refold into the partial stable *tac* stem conformation (Fig. 1B). These findings strongly support the proposed folding pathway in which a translationally inactive metastable structure of the *tac* stem region finally refolds into the active stable conformation (Gultyaev et al., 1997).

## RESULTS

The *hok* and *pnd* gene systems encode mRNAs with the same overall folding pathway (Thisted et al., 1994a; Gultyaev et al., 1997). They both form stable *tac* stems in their mRNAs. However, due to a deletion, the *tac* stem of *pnd* is 58 nt instead of the 74 nt of *hok* (Figs. 4, 5). This more simple structure of both the stable and metastable form of the *pnd tac* stem makes it a good candidate for studying its structures and folding kinetics and for comparing these with those of the *hok tac* stem.

Two RNA fragments of 74 and 58 nt were synthesized by T7 RNA polymerase transcription, corresponding to the stable *tac* stems of the *hok* and *pnd* mRNAs, respectively, and indicated as $hok^{74}$ and $pnd^{58}$ RNA fragments. To establish whether these isolated *tac* stem fragments were able to fold into the correct stable structures, we initially analyzed these RNA fragments with UV melting experiments. The reason for this is that we used denaturing gel electrophoresis to purify the *hok* and *pnd* RNA fragments and such an isolation procedure can lead to misfolded structures (Walstrum & Uhlenbeck, 1990; Emerick & Woodson, 1993). The results obtained, for both *hok* and *pnd*, with the UV melting experiments were irreproducible, although less pronounced for *pnd*, suggesting that a fraction of the RNA fragments was kinetically trapped into alternative conformations (results not shown). To avoid these irregularities, the $hok^{74}$ and $pnd^{58}$ fragments were incubated overnight at 37 °C, allowing the putative misfolded structure to refold to the stable state (Fresco et al., 1966). After this preincubation, the melting experiments indeed yielded reproducible results, indicating that virtually all the alternatively folded structures were refolded into the single stable *tac* stem structures (Uhlenbeck, 1995; Brion & Westhof, 1997; Pan & Woodson, 1998).

### Structure probing of the *hok*$^{74}$ and *pnd*$^{58}$ stable *tac* stem-loops

The 74-nt RNA fragment corresponding to the 5′ end of the *hok* mRNA (Fig. 1D) was probed with three different RNases (nuclease S1, RNase T1, and V1) after overnight incubation at 37 °C in a 50 mM Na cacodylate buffer at pH 7.2. The results of the enzymatic probing experiments are depicted in Figure 2. The cleavage sites are superimposed on the secondary structure model of the stable *tac* stem as established by Thisted et al. (1994a, 1995), and Gultyaev et al. (1997) (Fig. 4A).

The stable structure of the *hok*$^{74}$ fragment consists of a single stem-loop with a large internal loop at the bottom of the hairpin, two bulge loops, and a U•U mismatch (Gultyaev et al., 1997). The structure of the established stable hairpin is supported by multiple RNase V1 cuts from U6 to G30 and to a lesser extent on the opposing strand from G47 to G71. RNase V1 cuts are also found in the internal loop that indicates that this region is in a stacked conformation probably due to the presence of four possible non-Watson–Crick G•A base pairs. This was further supported by the lack of nuclease S1 and RNase T1 cuts in this internal loop region. Only G67 and A68 give weak nuclease S1 cuts showing that the internal loop is only weakly accessible to these enzymes, if at all (Fig. 2A).

Interestingly, some weak nuclease S1 cuts are also found in the stem region at C16, U17, and G52. These cleavages could point to the existence of a small fraction of molecules that are in the metastable state, because these positions correspond to the loops of the metastable hairpins I and II as predicted by Thisted et al. (1995) and Gultyaev et al. (1997) (see below). This small fraction could be the result of either an equilibrium with the stable structure or an incomplete refolding after overnight incubation at 37 °C.

The top of the hairpin consists of a rather loose structure harboring a bulge loop from A31 to G33 and a hairpin loop structure of 4 nt from U38 to G41. The G•U-rich stem at the top of the hairpin is supported by RNase V1 cuts at position G34 to U38, which indicates that this part of the structure is stacked or base paired. However, clear nuclease S1 and RNase T1 cuts occur in this same region between G34 and U38 and in U42 to C45, which indicate structural flexibility in this region. The hairpin loop (U39 to G41) at the top of the stable hairpin is also clearly indicated by the presence of strong nuclease S1 and RNase T1 cleavages. Together these experimental data in the region between U38 and C45 support the proposed model of the top of the stable *hok tac* stem (Fig. 4A).

Similar results were obtained for the *pnd*$^{58}$ stable *tac* stem-loop, which consists of a bulged C4 residue and two symmetrical internal loops (Fig. 5A, Franch & Gerdes, 1996; Gultyaev et al., 1997). The bottom part of the stable structure of *pnd*$^{58}$ up to the first internal loop

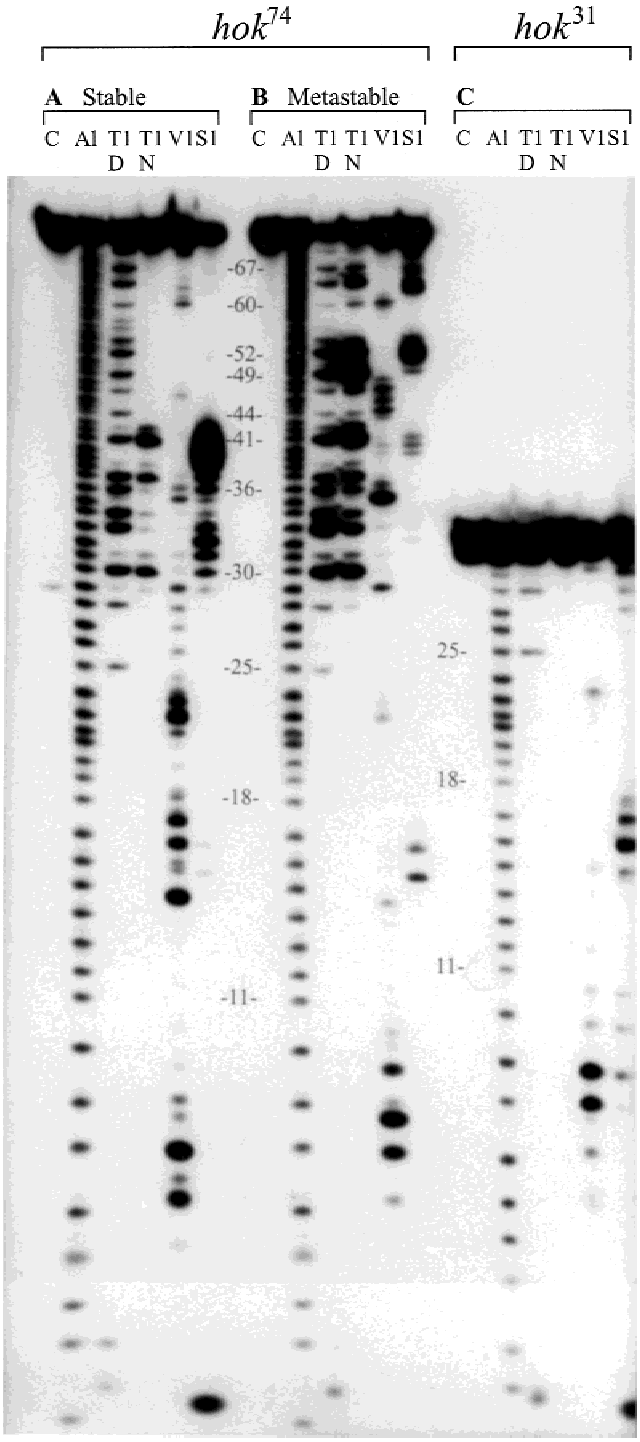


**FIGURE 2.** The enzymatic structure probing of the 5′ $^{32}$P-labeled *hok*$^{74}$ RNA fragment. **A**: Probing of the stable *hok*$^{74}$ *tac* stem structure. Prior to probing, the RNA was incubated overnight at 37 °C. **B**: Probing of the metastable *hok*$^{74}$ *tac* stem structure after heating and rapid cooling followed by probing at 0 °C. **C**: Probing of the *hok*$^{31}$ RNA fragment corresponding to the metastable hairpin I of the *hok*$^{74}$ RNA fragment. All probings were done in the sequence C (control), Al (alkaline hydrolysis), T1 D (RNase T1 under denaturing conditions), T1 N (RNase T1 under native conditions), V1 (RNase V1 under native conditions), and S1 (nuclease S1 under native conditions).

is confirmed by RNase V1 cuts, although nuclease S1 and RNase T1 cleavages do occur in this region as well, indicating some flexibility (Figs. 3A, 5A). Both internal loops are cleaved by RNase V1, indicating that these internal loops are partly in a closed or stacked conformation, probably due to the presence of G•A base pairs. However, the occurrence of nuclease S1 and RNase T1 cuts also indicates that these regions are not in a stable conformation. The stem region between the two internal loops (G12–G22 and C38–C48) is clearly supported by RNase V1 cuts at both the 3′ and 5′ half of the stem. The top of the hairpin, above the second internal loop, is probably not very stable because it is accessible to both nuclease S1 and RNase T1. The presence of RNase V1 cuts, however, is consistent with the top two base pairs of the proposed structure (Fig. 5A). Furthermore, the strong nuclease S1 cleavages in the region corresponding to the hairpin loop (G28-U32) favor the proposed hairpin structure of the stable *pnd*$^{58}$ *tac* stem significantly (Figs. 3A, 5A).

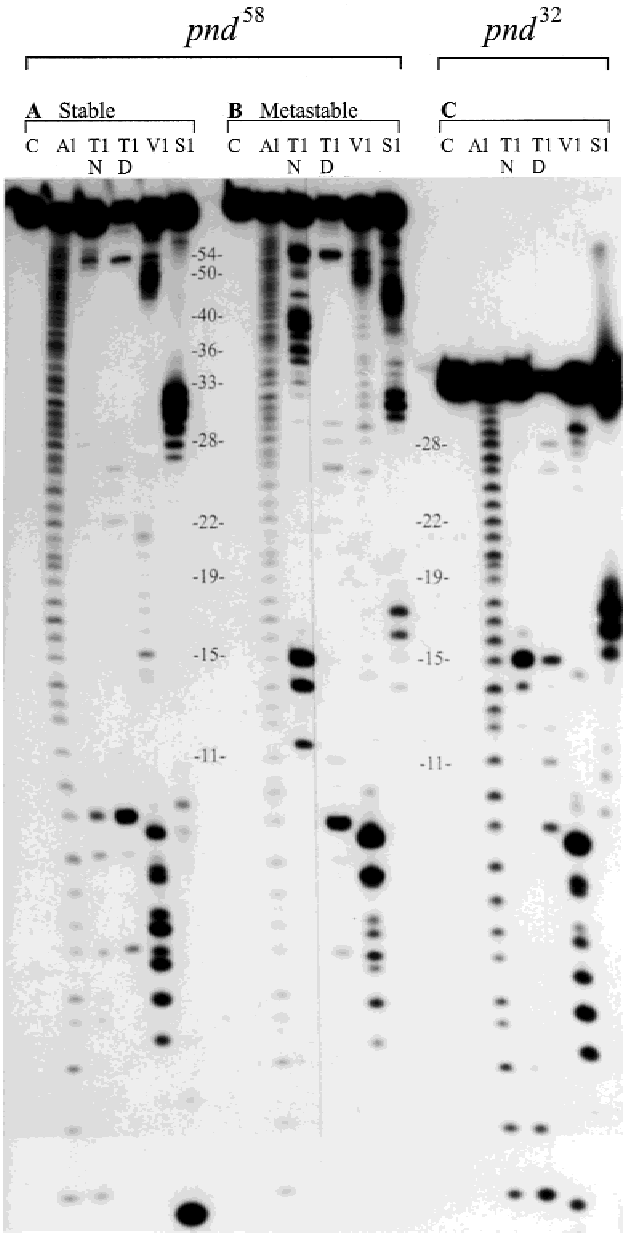


**FIGURE 3.** The enzymatic structure probing of the 5′ $^{32}$P-labeled *pnd*$^{58}$ RNA fragment. **A**: Probing of the stable *pnd*$^{58}$ *tac* stem structure. Prior to probing, the RNA was incubated overnight at 37 °C. **B**: Probing of the metastable *pnd*$^{58}$ *tac* stem structure after heating and rapid cooling followed by probing at 0 °C. **C**: Probing of the *pnd*$^{32}$ RNA fragment corresponding to the metastable hairpin I of the *pnd*$^{58}$ RNA fragment. All probings were done in the sequence C (control), Al (alkaline hydrolysis), T1 N (RNase T1 under native conditions), T1 D (RNase T1 under denaturing conditions), V1 (RNase V1 under native conditions), and S1 (nuclease S1 under native conditions).

## The *hok*$^{74}$ and *pnd*$^{58}$ metastable *tac* structures

To entrap the *hok*$^{74}$ *tac* stem fragment into the metastable structure, we first had to create a kinetic trap that would force the *tac* stem region into the metastable state that, second, should exist long enough to be able to probe this structure correctly. To fulfill these two requirements, the *hok*$^{74}$ *tac* stem fragment was first heated to 95 °C in a 50-mM Na cacodylate buffer, pH 7.2, for 2 min, followed by rapidly cooling to −180 °C by placing the RNA solution into liquid nitrogen. After thawing, the *hok*$^{74}$ *tac* stem fragment was probed at 0 °C with nuclease S1, RNase T1, and RNase V1. In this way the heating and rapid cooling cycle meets the first requirement, which allows the *hok*$^{74}$ RNA fragment to fold into the metastable state, if the metastable state folds faster than the stable state. The probing at 0 °C fulfilled the second requirement, because no significant refolding into the stable state was observed during the probing experiment as shown in Figure 2B. Under these conditions we were able to determine the structure of the metastable state of the *hok*$^{74}$ *tac* stem fragment and to overlay the probing results on the metastable structure as predicted by Gultyaev et al. (1997) (Fig. 4B).

The metastable structure of the *hok*$^{74}$ fragment consists of two hairpins, I and II (Fig. 4B). The top of hairpin II corresponds to the hairpin predicted by Gultyaev et al. (1997). However, the 3′-end nucleotides in the predictions are base-paired to a downstream part of the *hok* mRNA, which is not present in the *hok*$^{74}$ fragment. Therefore, this bottom part of hairpin II is referred to as the extended part of hairpin II indicated as II* (Fig. 4B).

A probing pattern completely different from the stable structure was obtained with the heated and rapidly cooled RNA fragment. The probing pattern consisted of RNase V1 cleavages in the region from U7 to C12 and from A23 and U29. This combined with strong nuclease S1 cuts in the region from U14 to U17 confirmed the existence of the metastable hairpin I. Here again, the internal loop seems to be inaccessible to both nuclease S1 and RNase T1 (Fig. 2B).

Hairpin II is supported by the V1 cuts at position G44 to U48 and in the opposing strand at A59 and G60.

Further confirmation of the existence of hairpin II comes from the strong nuclease S1 and RNase T1 cuts in the five-membered hairpin loop. This hairpin loop might be partially extended by 4 nt upon disruption of the two G•U base pairs as indicated by the presence of nuclease S1 and RNase T1 cuts at G47 and G54.

The extended part of hairpin II seems to be unstable, as both nuclease S1 and RNase T1 are able to cut at various positions in this stem region. However, RNase V1 cuts in the same region supports the existence of stacked or base-paired interactions in this region. Moreover, the proposed interactions are also supported by computer predictions of the secondary structure of the *hok*$^{74}$ fragment. Furthermore, the symmetrical internal loop connecting hairpin II and the extended II* region is clearly visible as a strong set of bands in the autoradiogram, suggesting that this area is more exposed to nuclease S1 and RNase T1 than the suggested base-paired region of stem II* (Figs. 2B, 4B).

As an additional control, an RNA fragment corresponding to the 5′-terminal 31 nt of the *hok*$^{74}$ *tac* stem region was also synthesized. This *hok*$^{31}$ fragment could further support the existence of a metastable structure in the *hok*$^{74}$ fragment, because it can only fold into the same structure as hairpin I of the metastable structure of *hok*$^{74}$.

A close resemblance between the cleavage pattern of the *hok*$^{31}$ fragment and the 5′-proximal region of *hok*$^{74}$ in the metastable state was indeed observed (Fig. 2B,C). This is especially true for the RNase T1 and V1 probes used. The only difference observed is the strong nuclease S1 cut at G1 and weaker cuts at U7 to G10 and A26 to U29. The reason why the strong nuclease S1 cut at G1 is present in the *hok*$^{31}$ fragment but not in the metastable *hok*$^{74}$ fragment is because the *hok*$^{31}$ fragment is extended by 1 nt at the 5′ end (G1). Therefore, the pattern on the gel is shifted upwards by 1 nt (Fig. 2C). The weak nuclease S1 cuts in U7 to G10 and in A26 to U29 are missing in the metastable state of the *hok*$^{74}$ fragment. This indicates that the stem-loop structure of the *hok*$^{31}$ fragment has a lesser overall stability than the stem-loop structure of hairpin I of the *hok*$^{74}$ fragment (Fig. 2B,C).

The V1 cuts from U6 to U15 and from the opposing strand C22 and A23 are in agreement with the existence of the stem-loop structure in *hok*$^{31}$. These cuts are nearly identical to the V1 cuts in the metastable hairpin I of the *hok*$^{74}$ *tac* stem fragment. The hairpin loop of the *hok*$^{31}$ fragment is also clearly visible with the nuclease S1 cuts from U15 to G18. The overall probing pattern of the *hok*$^{31}$ fragment corresponds well with the pattern from the hairpin I of the metastable state of the *hok*$^{74}$ fragment, further confirming the existence of the metastable state in the latter.

To determine the metastable structure of the *pnd*$^{58}$ *tac* stem, the same procedure of heating and rapid cooling was used as for the *hok*$^{74}$ fragment. However, to our surprise, the metastable state of the *pnd*$^{58}$ *tac* stem could not be formed using the same buffer of 50 mM Na cacodylate, pH 7.2. The reason for this behavior was inferred from UV melting experiments (data not shown), indicating that the stable *pnd tac* stem did not completely unfold at 95 °C in this buffer. Reducing the salt concentration to 0.5 mM solved this problem, because the melting temperature of the stable *tac* stem structure was lowered to 78 °C. A heating and rapid cooling cycle under these conditions enabled us to probe the metastable structure of the *pnd tac* stem (Fig. 3).

The metastable state of the *pnd*$^{58}$ *tac* stem was predicted to consist of a single hairpin with an internal loop of four bases comprising two A•G mismatches (Fig. 5B). The remainder of the sequence is in a more or less single-stranded state. Although several alternative structures can be formed in the region from U32 to C58, none of them is very stable. The most likely alternative secondary structure of this region, in agreement with the experimental data, is shown in Figure 5B.

The RNase V1 cuts from C4 to G11 and at G22, A23, G26 to U29, and U31 support the existence of the metastable hairpin. This hairpin structure is further supported by strong nuclease S1 and RNase T1 cuts in the loop of this hairpin. The weak RNase V1 cuts from U14 to U18 indicate the presence of a small fraction of the RNA fragments in the stable state, as these RNase V1 cuts are absent in the *pnd*$^{32}$ control hairpin (see below).

Analogous to the *hok*$^{31}$ fragment, we synthesized a 32-nt fragment corresponding to the 5′ end of *pnd*$^{58}$ that can only fold into the same hairpin as the 5′-proximal hairpin of the metastable state of the *pnd*$^{58}$ *tac* stem fragment (Fig. 5B).

Figure 3C shows the results of the structure mapping of *pnd*$^{32}$. RNase V1 cuts from position G3 to A10 and A25 to U29 support the existence of the stem. Evidence for this hairpin comes from the strong nuclease S1 and RNase T1 cuts in the region from G15 to U18, whereas the internal loop is supported by weak nuclease S1 and RNase T1 cuts in the region from G9 to G12. These results correspond very well with those found in the first 32 nt of the complete metastable *tac* stem, although the nuclease S1 cuts in the hairpin loop of the complete *tac* stem are less pronounced (Fig. 3).

### The kinetic transition of the metastable *tac* stems of *hok*$^{74}$ and *pnd*$^{58}$

To determine whether the metastable *hok*$^{74}$ *tac* stem is able to refold into the stable *tac* stem, a kinetic nuclease S1 probing experiment was performed (see Materials and Methods). The *hok*$^{74}$ fragment was subjected

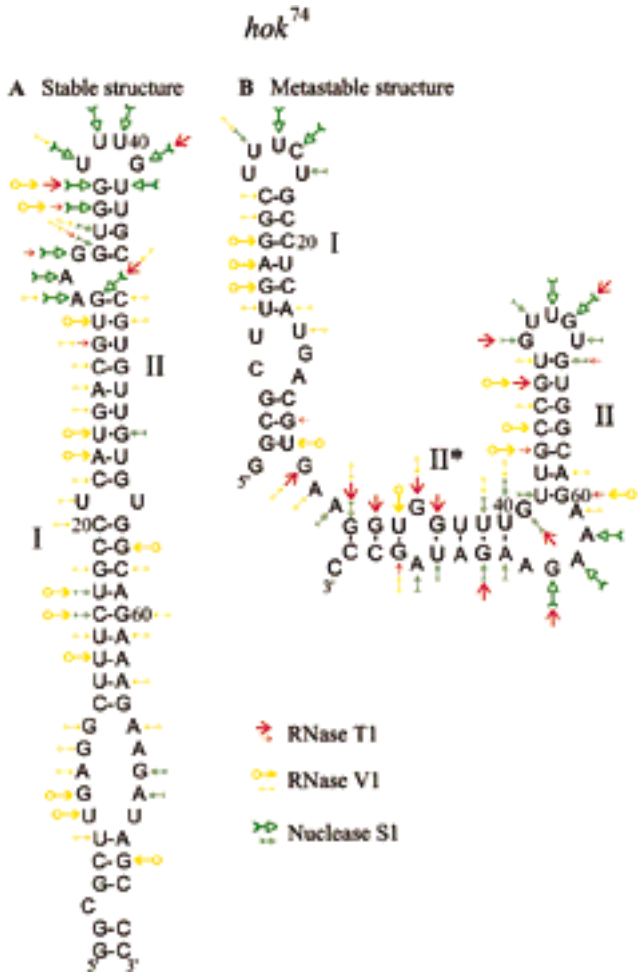


**FIGURE 4.** Summary of the structure probing results of the *hok*[74] RNA fragment. **A**: The stable structure. **B**: The metastable structure. Cleavage sites are indicated by arrows (RNase T1 in red, RNase V1 in yellow, and nuclease S1 in green). The larger arrows correspond to major cuts and the small arrows to minor cuts.

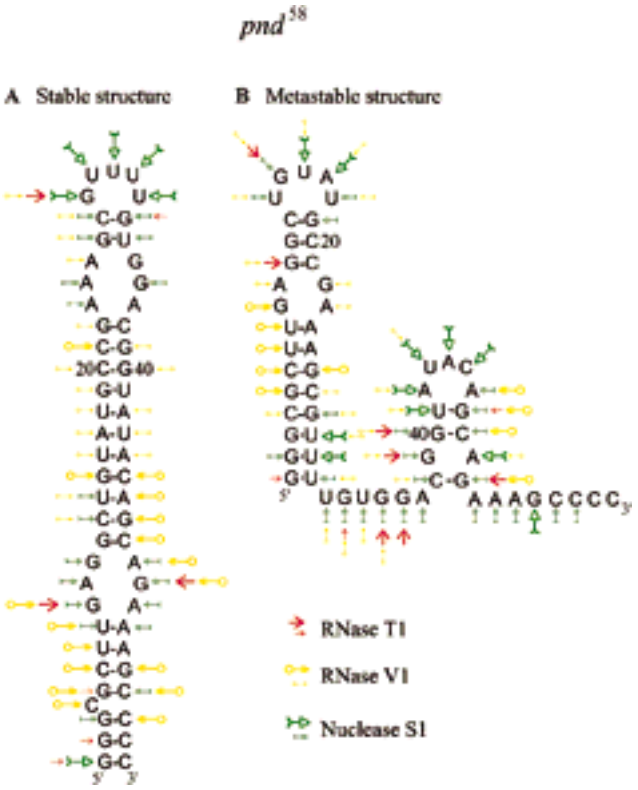


**FIGURE 5.** Summary of the structure probing results of the *pnd*[58] RNA fragment. **A**: The stable structure. **B**: The metastable structure. Cleavage sites are indicated by arrows (RNase T1 in red, RNase V1 in yellow, and nuclease S1 in green). The larger arrows correspond to major cuts and the small arrows to minor cuts.

to the same heating and cooling procedure as described above. Kinetics of refolding was then followed at 30 °C in 50 mM Na cacodylate buffer, pH 7.2. At each time point, a sample was taken and probed at 0 °C (Fig. 6A).

The nuclease S1 cuts at positions U15, C16, U50 to U53, and A62 to G64, representative of the metastable state, are clearly visible at $t = 0$ min. Over time these bands slowly diminish in intensity and at $t = 100$ min they have disappeared, as is the case for the overnight incubation at 37 °C, which is representative of the presence of the stable state. The weak nuclease S1 cuts at position U39 to U42 at $t = 0$ min clearly increase in intensity and become comparable to those for the stable state after ~100 min (Fig. 6A).

These results clearly show that refolding from the metastable to the stable state occurs in the *hok*[74] fragment. The refolding under these in vitro conditions seems sufficiently slow to allow the metastable state to exist until the complete *hok* mRNA is synthesized, thereby preventing the premature formation of the stable *tac* stem.

In the same way as with *hok*[74] fragment, the kinetics of the transition from the metastable to the stable state was determined for the *pnd*[58] *tac* stem, except that the incubation temperatures were 15 and 20 °C instead of 30 °C (Fig. 6B).

The strong nuclease S1 cuts in the region from U14 to A17, G40 to C45, and at position A49 and G54 clearly disappear in time. After 60 min at 15 °C the intensities for the cleavages observed are comparable with those for the stable state (see lane o/n in Fig. 6B). The strong nuclease S1 cuts from U29 to U31 did not increase over time. This could be an indication that this region is accessible to nuclease S1 in both states (Fig. 6B).

At 20 °C, the same kinetics could be observed, although the transition rate was much faster than expected as compared to 15 °C (Fig. 6B). The overall rate was estimated to be increased fivefold going from 15 to 20 °C. A further decrease in rate of about five times at 10 °C was observed (data not shown). At 0 °C no transition could be detected even after 2 h of incubation. This indicates that the probing at 0 °C after incubation at 15 or 20 °C does not influence the determined kinetics at elevated temperatures. Similar results were observed for *hok*[74], although less pronounced.

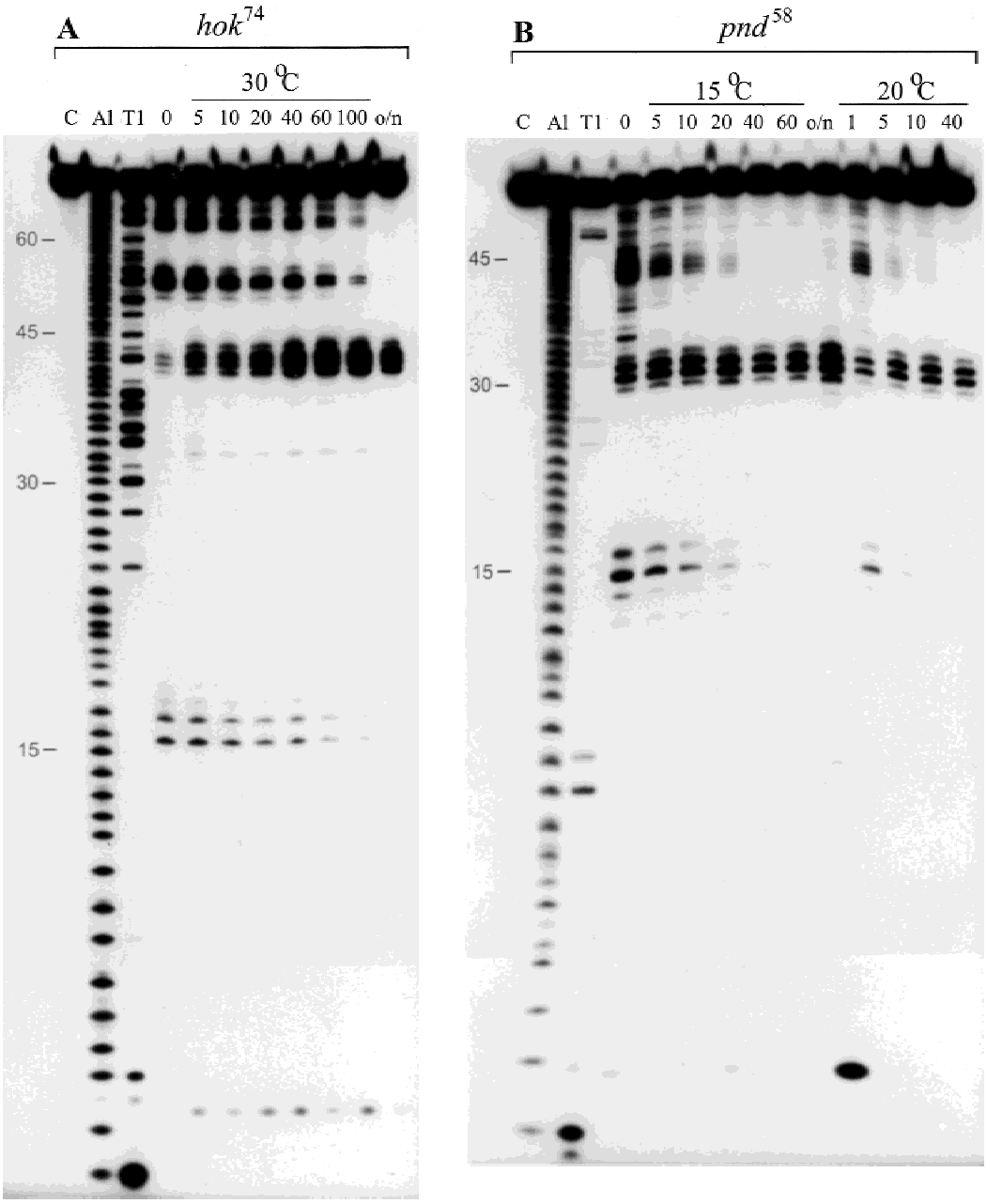


**FIGURE 6.** Kinetics of refolding of the metastable to the stable structures of the *hok*[74] and *pnd*[58] RNA fragments, followed by nuclease S1 probing. **A**: Heated and rapidly cooled *hok*[74] RNA was incubated at 30 °C in 50 mM Na cacodylate for various periods of time as indicated and subsequently probed at 0 °C with nuclease S1. C: control, Al: alkaline hydrolysis, T1: RNase T1 under denaturing conditions, and o/n: probing after overnight incubation at 37 °C. **B**: Heated and rapidly cooled *pnd*[58] RNA was incubated at 15 and 20 °C in 50 mM Na cacodylate for various periods of time as indicated and subsequently probed at 0 °C with nuclease S1. C: control, Al: alkaline hydrolysis, T1: RNase T1 under denaturing conditions, and o/n: probing after overnight incubation at 37 °C.

## DISCUSSION

A metastable structure at the 5′ end of *hok* mRNA and related messengers was predicted by Gultyaev et al. (1997) using a genetic algorithm, which is able to simulate the folding pathway of a growing RNA chain. The two 5′-terminal hairpins in the leader of the *hok* mRNA, also supported by sequence comparison, were shown to be transiently folded and replaced at the end of transcription by the more stable structure. The latter structure consists of an interaction between the very 5′ and 3′ ends (*tac*/*fbi* pairing) and the partial formation of the *tac* stem in the untranslated region (Fig. 1B). In this way, premature translation of the plasmid-mediated toxin is prevented in the full-length mRNA. The mRNA is activated by 3′-end processing that removes the *fbi*-

sequence, and this allows for the formation of the complete *tac* stem (Fig. 1C) (Thisted et al., 1994a; Franch & Gerdes, 1996; Franch et al., 1997).

Here we show that this 5′-terminal metastable structure exists indeed in a short RNA fragment corresponding to the *tac* stem and containing 74 and 58 nt in *hok* and *pnd*, respectively. To establish the occurrence of this metastable state, it was necessary to kinetically trap this structure by performing a heating and rapid cooling cycle procedure (Emerick & Woodson, 1994; Poot et al., 1997). Such a cycle yields almost 100% of the metastable structure, which also persists long enough at 0 °C to allow structure probing at this temperature. To our surprise, the *tac* stem fragment of *pnd* required heating at 95 °C at much lower salt concentrations to trap the metastable conformation. The reason for this was that the stable structure of the *pnd* fragment could not be melted completely at higher salt concentrations, as shown by UV melting experiments. On the other hand, the stable *tac* stem conformation could be obtained relatively easily by incubating the RNA overnight at 37 °C both in the case of the $hok^{74}$ and the $pnd^{58}$ molecules. This stable equilibrated structure, corresponding to one single long hairpin, was unambiguously proven with RNase probing experiments.

Both the overnight incubation and the heating and rapid cooling procedure allowed us to perform kinetic experiments to follow the structural transition from the metastable to the stable state. These experiments showed that the metastable states of $hok^{74}$ and $pnd^{58}$ could refold to the stable structures in a time scale of minutes to hours at temperatures that are close to physiological conditions. The estimated half-lives as determined on the basis of the autoradiograms of the probing experiments in the refolding buffer of 50 mM Na cacodylate, pH 7.2, were approximately 10 min at 30 °C for $hok^{74}$ and 4–5 min at 15 °C for $pnd^{58}$. However, at 20 °C the half-life of the metastable structure of $pnd^{58}$ appeared to be less than 1 min, which is approximately five times faster than at 15 °C. This corresponds to an estimated activation energy of about 50 kcal $mol^{-1}$ (Gutfreund, 1995). For $hok^{74}$, a similar but smaller increase in rate with temperature elevation was observed. Both the differences in refolding rates of $hok^{74}$ and $pnd^{58}$ and their temperature dependence seem to be inconsistent with the assumption that complete unfolding of the metastable hairpins of both $hok^{74}$ and $pnd^{58}$ must take place before a refolding into the stable structures is possible, as was found, for instance, for the MDV-1 (−) RNA products (Kramer & Mills, 1981). This would require a much larger activation energy: in the case of $pnd^{58}$ the complete disruption of the metastable stem requires an activation energy of about 100 kcal $mol^{-1}$, as calculated by using parameters determined by D. Turner and co-workers (http://www.ibc.wustl.edu/~zuker/rna/energy/node5.html; Freier et al., 1986). Therefore, it may well be that only a partial unfolding of the metastable hairpins I (Figs. 1, 5) is the rate-limiting step in the refolding pathway to the stable *tac* stem.

In this model, it is likely that the bottom of the metastable hairpins I should unfold, allowing base pairing of the 3′ end with the now accessible 5′ end. This, in turn, could be followed by unfolding or branch migration of the top part of the metastable hairpin I, leading to the formation of the complete and stable *tac* stem of $hok^{74}$ and $pnd^{58}$. This is similar to what was suggested for the refolding induced by the *tac*/*fbi* interaction in the full-length mRNA (Franch & Gerdes, 1996). Such a gradual displacement of helices was also proposed for the P1/P-1 region of the *Tetrahymena* group I intron (Cao & Woodson, 1998). However, one might still expect $hok^{74}$ to refold faster than $pnd^{58}$, because unfolding of the bottom part of hairpin I in the *hok* fragment seems to require considerably less energy than that of the *pnd* fragment, as the internal loop is only three base pairs from the end of the stem (Fig. 4B). On the other hand, to allow the 3′-to-5′-end interaction in the $hok^{74}$ fragment that leads to the formation of the initial part of the stable hairpin, the extended part of the second metastable hairpin II (II*; Fig. 4B) should also unfold at least partly. This effect could explain the slower refolding rate of $hok^{74}$ compared to that of $pnd^{58}$. A similar model was suggested for the unfolding of the 58-nt domain between positions 1051 and 1108 of the 23S ribosomal RNA (Laing & Draper, 1994).

Another possible type of conformational change with characteristics of a branch migration mechanism has been proposed for the conformational switch in the spliced leader of *Leptomonas collosoma* (LeCuyer & Crothers, 1993, 1994). In this system a pseudoknot is proposed that forms the initiation region for the strand displacement. A similar pseudoknot (between U13 and C16 and G60 and A63 for *hok* and G15 and U18 and A42 and C45 for *pnd*) may alternatively play an important role in initiating disruption of the metastable state of the *hok* and *pnd* RNA fragments. In contrast to the refolding initiation at the bottom of the metastable hairpins, such a mechanism would not require disruption of base pairs at the very first steps. In both these models, an intermediate structure should exist with partial disruption of the metastable state accompanied by a partial formation of the stable alternative.

As stated above, a strand displacement mechanism was suggested to be involved in the refolding of the metastable hairpins into the stable *tac*/*fbi* interaction keeping the *pnd* or *hok* mRNAs translationally inactive (Fig. 1B) (Franch & Gerdes, 1996). It is clear that the in vivo process of refolding during transcription (i.e., in the absence of the 3′-terminal *fbi*-element) should be slow compared to the transcription rate, because premature formation of the stable and translationally active *tac* stem is detrimental to the system (Fig. 1C). However, extrapolation of the refolding rates, determined in vitro

in this study, to 37 °C is hazardous for a number of reasons. The used RNA fragments have 3′ ends, which in the complete messenger become involved in base pairing interactions with downstream regions (Thisted et al., 1995). Moreover, the conditions used in our analysis are rather far from physiological, especially for the *pnd* fragment, and more quantitative systematic measurements, for example, in the presence of $Mg^{2+}$, are required.

The role of the metastable structure in the *tac* stem resembles that of the 5′-leader in bacteriophage MS2 RNA, which regulates the expression of the maturation (A) gene (Poot et al., 1997). In both cases the metastable structures are formed during RNA transcription, allowing ribosomes to bind in the case of the 5′ leader in MS2 RNA and preventing premature binding in the case of *hok* and *pnd*. Although the structure of the metastable folding of the MS2 RNA is not elucidated, the direct measurements of the slow kinetics by ribosomal binding are evidence for its existence. Eventually in both cases, a stable conformation is formed, preventing further ribosome binding to the 5′ leader of MS2 RNA and allowing antisense Sok-RNA or ribosomes to bind to the *hok* mRNA. Other systems in which metastable secondary structures play an important role are, for instance, branched folding versus the rod-like structure in potato spindle tuber viroid RNA (Loss et al., 1991) and the copy number regulation in the *Escherichia coli* plasmid ColE1 (Gultyaev et al., 1995b). Metastable RNA structures are also important in the case for two Q$\beta$ replicase templates, MNV-11 and SV-11 (Biebricher & Luce, 1992; Gultyaev et al., 1995a). In these two systems the metastable structures allow RNA replication, which is blocked by the stable structure.

Here, we have obtained clear evidence for the existence of the metastable structure in the *tac* stem region in both *hok* and *pnd* mRNAs in vitro. The system also allowed us to glimpse the refolding rates and mechanism involved, and the first data obtained are consistent with the expected role of these metastable structures in vivo. However, determination of accurate kinetics and mutational analysis in vitro together with a functional analysis in vivo are needed. It will be interesting to see how this structural transition is fine-tuned and which mechanism is prevalent.

In any case, the 5′ terminal leader of *hok* and *pnd* mRNA provides us with an excellent tool to study secondary structural transitions in RNA in which complete hairpins with relatively low free energies are disrupted in favor of an alternative, even more stable, and completely different secondary structure. In more general terms it may add to our understanding of the formation of alternative structures during RNA transcription (Kramer & Mills, 1981; Ma et al., 1994; Gultyaev et al., 1997), and to our insight into the folding kinetics of RNA (Brion & Westhof, 1997).

## MATERIALS AND METHODS

### Bacterial strains and plasmids

For plasmid isolation and cloning, *E. coli* strain JM 101 was used in combination with the cloning vector pUC19. Isolation was done according to the Qiagen protocol. The purified plasmid clones of $hok^{74}$, $hok^{31}$, $pnd^{58}$, and $pnd^{32}$ were used in a $T_7$ RNA polymerase run of assay to harvest the RNA fragments.

### Cloning protocol for the RNA fragments

The DNA of the $hok^{74}$ fragment for cloning was isolated using the polymerase chain reaction (PCR) method with an extended 5′-end primer that contains the $T_7$ promoter and an *Eco*RI site. The template DNA used in the PCR was plasmid pBR322, which carries the 580-bp wt *hok*/*sok* system cloned between the *Eco*RI and *Bam*HI sites (pPR633; Gerdes et al., 1986; Thisted et al., 1994a). The isolated DNA from the PCR was cloned into the pUC19 plasmid between the *Eco*RI and *Sma*I sites. The DNA for cloning into the pUC19 plasmid for the $hok^{31}$, $pnd^{58}$, and $pnd^{32}$ was obtained by hybridizing two primers (Gibco BRL) containing the desired sequence together and ligating them to a $T_7$ promoter sequence that contained a partial *Hin*dIII site. These DNA fragments were cloned into pUC19 between the *Hin*dIII and *Eco*RI and *Sma*I and *Pst*I sites, respectively.

### RNA synthesis via $T_7$ RNA polymerase transcription

For the isolation of the RNA fragments of $hok^{74}$, $hok^{31}$, $pnd^{58}$, and $pnd^{32}$, purified pUC19 DNA was first linearized by *Sma*I for $hok^{74}$ and $pnd^{58}$, *Dra*I for $pnd^{32}$, and *Eco*RI for $hok^{31}$. The $hok^{31}$-linearized plasmid was made blunt ended by incubating it with 2 U of nuclease S1 (see Secondary structure probing on following page) at 37 °C for 60 min. The blunt-end plasmids were then used for a run-off $T_7$ RNA polymerase transcript assay. The $T_7$ RNA polymerase transcription was done in a buffer containing 200 mM HEPES at pH 7.5, 30 mM $MgCl_2$, 2 mM spermidine, 40 mM dithiothreitol (DTT), 24 mM of each NTP, and 3.6 U/$\mu$l of $T_7$ RNA polymerase. This was incubated for 4 h at 37 °C. The plasmid DNA concentration in the $T_7$ RNA polymerase assay was in all cases 0.1 $\mu$g/$\mu$L.

### 5′-end $^{32}$P labeling of RNA

The RNA was dephosphorylated with calf intestinal alkaline phosphatase (1 U/50 $\mu$L) from Pharmacia in a one-for-all buffer (Pharmacia) for 30 min at 37 °C, and then purified by phenol extraction and precipitated by ethanol. The 5′-end labeling was done in 1× one-for-all buffer with 0.95 U of T4 polynucleotide kinase (Pharmacia) and incubated for 45 min at 37 °C.

### Heating and rapid cooling experiment

The heating and rapid cooling experiment for $hok^{74}$ and $pnd^{58}$ *tac* stem fragment was done in 50 mM and 0.5 mM Na cac-

odylate buffer at pH 7.2, respectively. First the sample was heated at 95 °C for 2 min and then directly placed into liquid nitrogen. After this, the sample was carefully melted and used for probing and kinetic studies.

### Secondary structure probing using nuclease S1 and RNase T1 and V1

Structure probing with RNase T1 and V1 under native conditions was performed in 10 mM $MgCl_2$, 10 $\mu$g tRNA, and 50 mM Na cacodylate buffer at pH 7.2. The enzyme concentrations were 0.5 U and 0.01 U and 5 U and 0.08 U in 50 $\mu$L at 37 °C and 0 °C, respectively. The incubation times were 15 and 20 min at 37 °C and 0 °C, respectively. Nuclease S1 probing was in 0.2 M NaCl, 50 mM Na acetate, pH 4.5, 1 mM $ZnSO_4$, 0.5% glycerol, 10 $\mu$g tRNA and 2 or 8 U of enzyme in 30 $\mu$L at 37 °C or 0 °C, respectively. Incubation times were 10 and 20 min, respectively. Digestion with RNase T1 under denaturing conditions was in 6 $\mu$L of 0.4% (w/v) Na citrate·$2H_2O$, 0.14% (w/v) citric acid, 8 M urea, 0.4% (w/v) ethylene diamine tetraacetic acid (EDTA), and 10 $\mu$g tRNA + 3$\mu$L sample RNA ($^{32}$P 5′-end labeled), and the mixture was preincubated for 15 min at 55 °C. Then 1.5 $\mu$L of RNase T1 (1 U) was added and incubated for 20 min at 55 °C. The alkaline ladder was made from sample RNA in a 25-mM $Na_2CO_3$/$NaHCO_3$ (1/9) buffer for 2 min at 95 °C. All probing results were loaded on 20% polyacrylamide sequencing gels, containing 8 M urea, and detection was by autoradiography.

### Kinetic probing experiments

Kinetic experiments were performed in 50 mM Na cacodylate buffer at pH 7.2. Incubation was at 15, 20, or 30 °C in a PCR mini Cycler from MJ Research at various periods of time. Samples were taken and added to a pre-cooled 0.2 M NaCl, 50 mM Na acetate, pH 4.5, 1 mM $ZnSO_4$, 0.5% glycerol buffer with 8 U of nuclease S1. Probing was at 0 °C on ice for 20 min followed by analysis with electrophoresis on a 20% polyacylamide sequence gel containing 8 M urea.

## ACKNOWLEDGMENTS

We thank one of the anonymous referees for his/her remarks on the calculation of the activation energy. This work was partly supported by the EU (Biotech Program B104-98-0189).

*Received April 19, 1999; returned for revision June 7, 1999; revised manuscript received July 29, 1999*

## REFERENCES

Biebricher CK, Luce R. 1992. In vitro recombination and terminal elongation of RNA by Q$\beta$ replicase. *EMBO J 11*:5129–5135.

Brion P, Westhof E. 1997. Hierarchy and dynamics of RNA folding. *Annu Rev Biophys Biomol Struct 26*:113–137.

Cao Y, Woodson SA. 1998. Destabilizing effect of an rRNA stem-loop on an attenuator hairpin in the 5′ exon of the *Tetrahymena* pre-rRNA. *RNA 4*:901–914.

Emerick VL, Woodson SA. 1993. Self-splicing of the *Tetrahymena* pre-rRNA is decreased by misfolding during transcription. *Biochemistry 32*:14062–14067.

Emerick VL, Woodson SA. 1994. Fingerprinting the folding of group I precursor RNA. *Proc Natl Acad Sci USA 91*:9675–9679.

Franch T, Gerdes K. 1996. Programmed cell death in bacteria: Translational repression by mRNA end-pairing. *Mol Microbiol 21*:1049–1060.

Franch T, Gultyaev AP, Gerdes K. 1997. Programmed cell death by *hok*/sok of plasmid R1: Processing at the *hok* mRNA 3′ end triggers structural rearrangements that allow translation and antisense RNA binding. *J Mol Biol 273*:38–51.

Freier SM, Kierzek P, Jaeger JA, Sugimoto N, Caruthers MH, Nielson T, Turner DH. 1986. Improved free-energy parameters for predictions of RNA duplex stability. *Proc Natl Acad Sci USA 83*:9373–9377.

Fresco JR, Adains A, Ascione R, Henley D, Lindahl T. 1966. Tertiary structure in transfer ribonucleic acids. *Cold Spring Harbor Symp Quant Biol 31*:527–537.

Gerdes K, Rasmussen PB, Molin S. 1986. Unique type of plasmid maintenance function: Post-segregational killing of plasmid-free cells. *Proc Natl Acad Sci USA 83*:3116–3120.

Gultyaev AP, Franch T, Gerdes K. 1997. Programmed cell death by *hok*/sok of plasmid R1: Coupled nucleotide covariations reveal a phylogenetically conserved folding pathway in the *hok* family of mRNAs. *J Mol Biol 273*:26–37.

Gultyaev AP, van Batenburg FHD, Pleij CWA. 1995a. The computer simulation of RNA folding pathways using a genetic algorithm. *J Mol Biol 250*:37–51.

Gultyaev AP, van Batenburg FHD, Pleij CWA. 1995b. The influence of a metastable structure in plasmid primer RNA on antisense RNA binding kinetics. *Nucleic Acids Res 23*:3718–3725.

Gutfreund H. 1995. *Kinetics for the life sciences (receptors, transmitters and catalysts).* Cambridge: Cambridge University Press.

Kramer FR, Mills DR. 1981. Secondary structure formation during RNA synthesis. *Nucleic Acids Res 9*:5109–5124.

Laing LG, Draper DE. 1994. Thermodynamics of RNA folding in a conserved ribosomal RNA domain. *J Mol Biol 237*:560–576.

LeCuyer KA, Crothers D. 1993. The *Leptomonas collosoma* spliced leader RNA can switch between two alternative structural forms. *Biochemistry 32*:5301–5311.

LeCuyer KA, Crothers D. 1994. Kinetics of an RNA conformational switch. *Proc Natl Acad Sci USA 91*:3373–3377.

Loss P, Schmitz M, Riesner D. 1991. Formation of a thermodynamically metastable structure containing hairpin II is critical for infection of potato spindle tuber viroid RNA. *EMBO J 10*:719–727.

Ma CK, Kolesnikow T, Rayner JC, Simons EL, Yim H, Simons RW. 1994. Control of translation by mRNA secondary structures: The importance of the kinetics of structure formation. *Mol Microbiol 14*:1033–1047.

Nielsen AK, Gerdes K. 1995. Post-segregational killing by *hok*-homolog *pnd* of plasmid R483: Two translational control elements in the *pnd* mRNA. *J Mol Biol 249*:270–282.

Pan J, Woodson SA. 1998. Folding intermediates of a self-splicing RNA: Mispairing of the catalytic core. *J Mol Biol 280*:597–609.

Poot RA, Tsareva NV, Boni IV, van Duin J. 1997. RNA folding kinetics regulates translation of phage MS2 maturation gene. *Proc Natl Acad Sci USA 94*:10110–10115.

Thisted T, Gerdes K. 1992. Mechanism of post-segregational killing by the *hok7sok* system of plasmid R1: Sok antisense RNA regulates *hok* gene expression indirectly through the overlapping *mok* gene. *J Mol Biol 223*:41–54.

Thisted T, Nielsen AK, Gerdes K. 1994a. Mechanism of post-segregational killing: Translation of Hok, SrnB and Pnd mRNAs of plasmids R1, F and R483 is activated by 3′ end processing. *EMBO J 13*:1950–1959.

Thisted T, Sôrensen NS, Gerdes K. 1995. Mechanism of post-segregational killing: Secondary structure analysis of the entire Hok mRNA from plasmid R1 suggesting a fold-back structure that prevents translation and antisense RNA binding. *J Mol Biol 247*:859–873.

Thisted T, Sôrensen NS, Wagner EGH, Gerdes K. 1994b. Mechanism of post-segregational killing: Sok antisense RNA interacts with Hok mRNA via its 5′ end single stranded leader and competes with the 3′ end of Hok mRNA for binding to the mok translational initiation region. *EMBO J 13*:1960–1968.

Uhlenbeck OC. 1995. Keeping RNA happy. *RNA 1*:4–6.

Walstrum SA, Uhlenbeck OC. 1990. The self-splicing RNA of *Tetrahymena* is trapped in a less active conformation by gel purification. *Biochemistry 29*:10573–10576.